

Extension of the entropy viscosity method to the low Mach Euler equations and
the seven-equation two-phase model.

by
Marc-Olivier Delchini

August 4, 2014

Co-chairs: J. Ragusa¹ and J.L. Guermond².

Committee members: J. Morel¹, Y. Hassan¹ and R. Berry³.

Substitute: R. McClaren

¹Nuclear Engineering Department, Texas A&M University.

²Department of Mathematics, Texas A&M University.

³Idaho National Laboratory.

Outline:

- 1 Introduction
- 2 The multi-D Euler equations with variable area
 - Background
 - Low-Mach asymptotic limit
 - Numerical results
- 3 The multi-D seven-equation model with variable area
- 4 Conclusions and future work

Introduction

Why do we need to solve for conservation laws?

- Hyperbolic conservation laws → nuclear engineering, aeronautic, aerospace, oil engineering, ...
- Systems of equations that accurately describe the physical phenomena
- Need for accurate and robust modeling for engineering applications
- Require good understanding of the mathematical properties (eigenvalues, characteristic equations and variables , shock formation, ...)
- Numerical stabilizations: approximate Riemann solvers (HLL, HLLC), flux limiters, artificial dissipative methods (explicitly add the artificial dissipative terms), ...

Some mathematical properties

Let us consider a hyperbolic conservation law of the form:

$$\partial_t \vec{U} + \vec{\nabla} \cdot \vec{F}(\vec{U}) = \vec{0} \text{ (strong form)}$$

- wave-dominated problem \rightarrow eigenvalues
- known to form shocks even with smooth initial conditions: characteristic equations and variables, Riemann invariants
- uniqueness of the weak solution is ensured by an **entropy condition**: the associated entropy equation satisfies an inequality and is *peaked in the shock region*.

$$\partial_t S(\vec{U}) + \vec{\nabla} \cdot \vec{\Psi}(\vec{U}) \geq 0 \text{ entropy inequality}$$

S : physical entropy

$(S, \vec{\Psi})$ is an entropy pair

The general idea behind the entropy viscosity method

It is an artificial dissipation method with smart viscosity coefficient(s) capable of tracking the shock so that dissipation is only added into the shock region.

- it is a viscous regularization technique: the dissipative terms are consistent with the entropy inequality.
- each viscosity coefficient is function of a high-order viscosity coefficient and an upper bound called first-order viscosity coefficient.
- the high-order viscosity coefficient is defined proportional to the entropy residual.
- the first-order viscosity coefficient is function of the local maximum eigenvalue.
- also accounts for the inter element jumps → make the definition of the viscosity coefficients also sensitive to discontinuities other than shock.

The Multiphysics Object-Oriented Simulation Environment (MOOSE)

- Explicit and implicit temporal integrators (first and second-order accuracy)
- Continuous and Discontinuous Galerkin Finite Element Method
- Mesh adaptivity, time step adaptivity
- Support parallel runs
- Built on PETSc and Libmesh
- For implicit solves, requires a preconditioner → either Finite Difference Preconditioner (FDP) or hard-coded preconditioner
- C++ language, open-source

All numerical solutions were run with BDF2 and linear test functions → second-order accuracy in time and space for smooth solutions only!

BurGer's Equation (BadGER)



A simple example of application of the EVM: the 1-D Burger's equation

The 1-D Burger's equation with its viscous regularization

$$\partial_t u(x, t) + \partial_x \left(\frac{u(x, t)^2}{2} \right) = \color{blue}{\partial_x (\mu(x, t) \partial_x u(x, t))}$$

Definition of the local viscosity coefficient $\mu(x, t)$

$$\mu(x, t) = \min(\mu_e(x, t), \mu_{max}(x, t))$$

$$\mu_{max}(x, t) = \frac{h}{2} |u(x, t)|$$

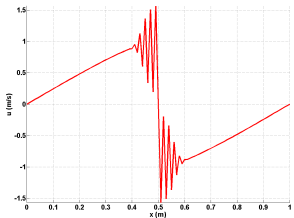
$$\mu_e(x, t) = h^2 \frac{\max(R(x, t), J)}{\|\eta(u) - \bar{\eta}(t)\|_\infty}$$

Entropy residual: $R(x, t) = \partial_t \eta(u) + \partial_x \Phi(u) \leq 0$

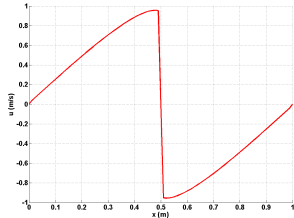
with $\eta(u) = u^2/2$ and $\Phi(u) = u^3/3$

Jump: $J = [[\partial_x \Phi(u)]]$

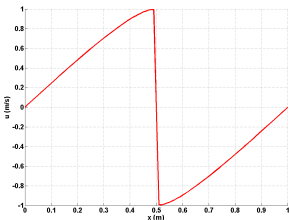
1-D numerical results (100 cells, CFL = 1 and $t_f = 0.24$ s)



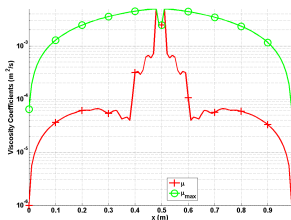
(a) Without stabilization.



(b) With first-order viscosity.



(c) With the EVM.



(d) Viscosity coefficient profiles.

The MULti-D Euler Equations with variable area (MULe DEEr)



Numerical methods for continuous and discontinuous schemes

- multi-wave problem, can develop shock waves and other types of discontinuities.
- Numerical methods for both continuous and discontinuous schemes: approximate Riemann solvers (HLL, HLLC, Roe scheme, · · ·), flux limiters , Lapidus viscosity, Pressure-based viscosity, SUPG, C-method, Entropy Viscosity Method (EVM).
- Numerical methods can be ill-scaled in the low-Mach limit, yielding the wrong incompressible system
- Low-Mach steady-state solution: time-dependent term preconditioner to accelerate the convergence of the solution to the steady-state (Turkel) when using an explicit scheme → the transient is no longer accurate. *Implicit solvers do not have this issue.*

The multi-D Euler equations with variable area

Mass conservation

$$\partial_t(\rho A) + \vec{\nabla} \cdot (\rho A \vec{u}) = 0$$

Momentum conservation

$$\partial_t(\rho \vec{u} A) + \vec{\nabla} \cdot (\rho A \vec{u} \otimes \vec{u} + P \mathbb{I}) = P \vec{\nabla} A$$

Energy conservation

$$\partial_t(\rho E A) + \vec{\nabla} \cdot [\vec{u} (\rho E + P) A] = 0$$

Equation of state

$$P = eos(\rho, e)$$

Multi-wave problem: $\lambda_1 = \vec{u} \cdot \vec{n} - c$, $\lambda_2 = \vec{u} \cdot \vec{n} + c$ and $\lambda_{3,\dots,3+D} = \vec{u} \cdot \vec{n}$.

The area A is only a function of space.

- The isentropic compressible multi-D Euler equations degenerate into an incompressible system in the low-Mach asymptotic limit.

$$\partial_t \rho + \vec{u} \cdot \vec{\nabla} \rho = 0$$

$$\partial_t \vec{u} + \vec{u} \cdot \vec{\nabla} \cdot \vec{u} + \frac{1}{\rho} \vec{\nabla} P = 0$$

$$\vec{\nabla} \cdot (\vec{u} A) = 0$$

$$P(\vec{r}) = P_0 + M^2 P_2(\vec{r})$$

- no energy equation since the flow is assumed isentropic
- pressure fluctuations of the order of the Mach number square *at steady state*

Objectives: extend the EVM to low-Mach flows while maintaining its capabilities of solving for transonic and supersonic flows, and use an implicit solver.

How to do it?

- ➊ recast the entropy equation as a function of the pressure, the density, the velocity and the speed of sound.

$$\mu_e(\vec{r}, t) = h^2 \frac{\max(R(\vec{r}, t), J)}{\|s - \bar{s}(t)\|_\infty}$$

- ➋ work with the non-dimensionalized version of the multi-D Euler equations in order to understand how the different terms scale
- ➌ derive a definition for the viscosity coefficients that ensures well-scaled dissipative terms for a wide range of Mach numbers

Recast the entropy residual

New entropy residual

$$D_e(\vec{r}, t) = \partial_t s + \vec{u} \cdot \vec{\nabla} s = \frac{s_e}{P_e} \underbrace{\left(\frac{dP}{dt} - c^2 \frac{d\rho}{dt} \right)}_{\tilde{D}_e(\vec{r}, t)} \rightarrow c^2 = \frac{dP}{d\rho}$$

The viscosity coefficients

- The viscosity coefficient will be set proportional to $\tilde{D}_e(\vec{r}, t)$ (instead of $D_e(\vec{r}, t)$):

$$\mu_e(\vec{r}, t) = h^2 \frac{\max(\tilde{D}_e(\vec{r}, t), J)}{\text{norm}_P^\mu} \text{ and } \kappa_e(\vec{r}, t) = h^2 \frac{\max(\tilde{D}_e(\vec{r}, t), J)}{\text{norm}_P^\kappa}$$

- $\tilde{D}_e(\vec{r}, t)$ is an alternative way of computing the local entropy production
- This new expression offers more diversity in the choice of the **normalization parameter** norm_P : P , ρc^2 , $\rho c \|\vec{u}\|$ or $\rho \|\vec{u}\|^2$

A viscous regularization for the multi-D Euler equations with variable area

Mass conservation

$$\partial_t(\rho A) + \vec{\nabla} \cdot (\rho A \vec{u}) = \vec{\nabla} \cdot \vec{f}$$

Momentum conservation

$$\partial_t(\rho \vec{u} A) + \vec{\nabla} \cdot (\rho A \vec{u} \otimes \vec{u} + P \mathbb{I}) = P \vec{\nabla} A + \vec{\nabla} \cdot \left(\mathbb{F}(\vec{u}) + \vec{u} \otimes \vec{f} \right)$$

Energy conservation

$$\partial_t(\rho E A) + \vec{\nabla} \cdot [\vec{u} (\rho E + P) A] = \vec{\nabla} \cdot \left(\vec{h} + \vec{u} \cdot \mathbb{F}(\vec{u}) + \frac{\|\vec{u}\|^2}{2} \vec{f} \right)$$

Dissipative terms

$$\vec{f} = A \kappa \vec{\nabla} \rho, \quad \vec{h} = A \kappa \vec{\nabla}(\rho e) \text{ and } \mathbb{F}(\vec{u}) = A \mu \vec{\nabla}^s \vec{u} \text{ or } \mathbb{F}(\vec{u}) = A \mu \vec{\nabla} \vec{u}$$

→ two positive viscosity coefficients μ and κ . Requires a concave physical entropy $s(\rho, e)$.

Non-dimensionalized multi-D Euler equations

We define some reference variables denoted by subscript ∞ :

$$\rho^* = \frac{\rho}{\rho_\infty}, \quad u^* = \frac{u}{u_\infty}, \quad P^* = \frac{P}{\rho_\infty c_\infty^2}, \quad E^* = \frac{E}{c_\infty^2},$$
$$x^* = \frac{x}{L_\infty}, \quad t^* = \frac{t}{L_\infty/u_\infty}, \quad \mu^* = \frac{\mu}{\mu_\infty}, \quad \kappa^* = \frac{\kappa}{\kappa_\infty}$$

→ μ_∞ and κ_∞ are function of the normalization parameters $norm_P^\mu$ and $norm_P^\kappa$, respectively. We also define the following reference numbers:

$$\text{Mach number: } M_\infty = \frac{u_\infty}{c_\infty},$$

$$\text{Numerical Reynolds number: } \text{Re}_\infty = \frac{u_\infty L_\infty}{\mu_\infty},$$

$$\text{Numerical P\'echlet number: } \text{P\'e}_\infty = \frac{u_\infty L_\infty}{\kappa_\infty},$$

Non-dimensionalized multi-D Euler equations

$$\partial_{t^*} \rho^* + \vec{\nabla}^* \cdot (\rho^* \vec{u}^*) = \frac{1}{\text{P\'{e}}_\infty} \vec{\nabla}^* \cdot (\kappa^* \vec{\nabla}^* \rho^*)$$

$$\begin{aligned} \partial_{t^*} (\rho^* \vec{u}^*) + \vec{\nabla}^* \cdot (\rho^* \vec{u}^* \otimes \vec{u}^*) + \frac{1}{M_\infty^2} \vec{\nabla}^* P^* &= \frac{1}{\text{Re}_\infty} \vec{\nabla}^* \cdot \left(\rho^* \mu^* \vec{\nabla}^{s,*} \vec{u}^* \right) \\ &\quad + \frac{1}{\text{P\'{e}}_\infty} \vec{\nabla}^* \cdot \left(\vec{u}^* \otimes \kappa^* \vec{\nabla}^* \rho^* \right) \end{aligned}$$

$$\begin{aligned} \partial_{t^*} (\rho^* E^*) + \vec{\nabla}^* \cdot [\vec{u}^* (\rho^* E^* + P^*)] &= \frac{1}{\text{P\'{e}}_\infty} \vec{\nabla}^* \cdot \left(\kappa^* \vec{\nabla}^* (\rho^* e^*) \right) \\ &\quad + \frac{M_\infty^2}{\text{Re}_\infty} \vec{\nabla}^* \cdot \left(\vec{u}^* \rho^* \mu^* \vec{\nabla}^{s,*} \vec{u}^* \right) + \frac{M_\infty^2}{2\text{P\'{e}}_\infty} \vec{\nabla}^* \cdot \left(\kappa^* (u^*)^2 \vec{\nabla}^* \rho^* \right) \end{aligned}$$

The above equations are valid for all-Mach flows.

For a low-Mach flow

→ choose Re_∞ and Pé_∞ so that we recover the incompressible equations in the low-Mach limit (pressure fluctuations and $\vec{\nabla} \cdot \vec{u}_0 = 0$).

- assume Ideal gas equation of state for simplicity: $P = (\gamma - 1)\rho e$
- expand each variable in powers of the Mach number:
$$P(\vec{r}, t) = P_0(\vec{r}, t) + P_1(\vec{r}, t)M_\infty + P_2(\vec{r}, t)M_\infty^2 + \dots$$
- choose $\text{Re}_\infty = \text{Pé}_\infty = 1$
- derive the leading, first and second-order momentum equations
- derive the leading-order energy and mass equations

For a low-Mach flow: momentum equation

$$\partial_t (\rho \vec{u}) + \vec{\nabla} \cdot (\rho \vec{u} \otimes \vec{u}) + \frac{1}{M_\infty^2} \vec{\nabla} P = \frac{1}{\text{Re}_\infty} \vec{\nabla} \cdot (\rho \mu \vec{\nabla}^s \vec{u}) + \frac{1}{\text{Pé}_\infty} \vec{\nabla} \cdot (\vec{u} \otimes \kappa \vec{\nabla} \rho)$$

Leading and first-order momentum equations:

$$\vec{\nabla} P_0 = \vec{\nabla} P_1 = 0 \longrightarrow P(\vec{r}) = \tilde{P}_0 + P_2(\vec{r}) M_\infty^2$$

Second-order momentum equation:

$$\partial_t (\rho \vec{u})_0 + \vec{\nabla} \cdot (\rho \vec{u} \otimes \vec{u})_0 + P_2 = \vec{\nabla} \cdot (\rho \mu \vec{\nabla}^s \vec{u})_0 + \vec{\nabla} \cdot (\vec{u} \otimes \kappa \vec{\nabla} \rho)_0$$

For a low-Mach flow: energy and mass equations

$$\begin{aligned}\partial_{t^*} (\rho^* E^*) + \vec{\nabla}^* \cdot [\vec{u}^* (\rho^* E^* + P^*)] &= \frac{1}{\text{Pé}_\infty} \vec{\nabla}^* \cdot (\kappa^* \vec{\nabla}^* (\rho^* e^*)) \\ &+ \frac{M_\infty^2}{\text{Re}_\infty} \vec{\nabla}^* \cdot (\vec{u}^* \rho^* \mu^* \vec{\nabla}^{s,*} \vec{u}^*) + \frac{M_\infty^2}{2\text{Pé}_\infty} \vec{\nabla}^* \cdot (\kappa^* (u^*)^2 \vec{\nabla}^* \rho^*)\end{aligned}$$

Leading-order energy equation:

$$\partial_t (\rho E)_0 + \vec{\nabla} \cdot [\vec{u} (\rho E + P)]_0 = \vec{\nabla} \cdot (\kappa \vec{\nabla} (\rho e))_0 \longrightarrow \vec{\nabla} \cdot \vec{u}_0 = 0$$

$$\partial_t \rho + \vec{\nabla} \cdot (\rho \vec{u}) = \frac{1}{\text{Pé}_\infty} \vec{\nabla} \cdot (\kappa \vec{\nabla} \rho)$$

Leading-order mass equation:

$$\partial_t \rho_0 + \vec{\nabla} \cdot (\rho \vec{u})_0 = \vec{\nabla} \cdot (\kappa \vec{\nabla} \rho)_0 \rightarrow \partial_t \rho_0 + \vec{u}_0 \vec{\nabla} \rho_0 = \vec{\nabla} \cdot (\kappa \vec{\nabla} \rho)_0$$

For a low-Mach flow: derivation of norm $_{P}^{\mu,\kappa}$

We were able to recover the incompressible equations by choosing $\text{Re}_{\infty} = \text{P\'{e}}_{\infty} = 1$. What does that imply for norm_{P}^{μ} and norm_{P}^{κ} ?

Derive an expression for κ_{∞} :

$$\kappa_e(\vec{r}, t) = h^2 \frac{\max(\tilde{D}_e(\vec{r}, t), J)}{\text{norm}_{P}^{\kappa}} \longrightarrow \kappa_{\infty} = \frac{\rho_{\infty} c_{\infty}^2 u_{\infty} L}{\text{norm}_{P,\infty}^{\kappa}}$$

Then, use the substitute the above expression for norm_{P}^{κ} into $\text{P\'{e}}_{\infty}$ to obtain:

$$\text{norm}_{P,\infty}^{\kappa} = \text{P\'{e}}_{\infty} \rho_{\infty} c_{\infty}^2 = \rho_{\infty} c_{\infty}^2$$

Same derivation using μ_e and Re_{∞} leads to:

$$\text{norm}_{P,\infty}^{\mu} = \text{Re}_{\infty} \rho_{\infty} c_{\infty}^2 = \rho_{\infty} c_{\infty}^2$$

For a non-isentropic flow, i.e., with shocks

- the flow can experience shocks and other waves → discontinuities
- the low-Mach asymptotic study is no longer valid
- directly work with the non-dimensionalized Euler equations
- determine the scaling of Re_∞ and Pé_∞ to stabilize the equations

For a non-isentropic flow: momentum equation

$$\partial_t (\rho \vec{u}) + \vec{\nabla} \cdot (\rho^* \vec{u} \otimes \vec{u}) + \frac{1}{M_\infty^2} \vec{\nabla} P = \frac{1}{\text{Re}_\infty} \vec{\nabla} \cdot (\rho \mu \vec{\nabla}^s \vec{u}) + \frac{1}{\text{Pé}_\infty} \vec{\nabla} \cdot (\vec{u} \otimes \kappa \vec{\nabla} \rho)$$

In the shock region, the term $\frac{1}{M_\infty^2} \vec{\nabla} P$ will become dominant and will need to be stabilized by a dissipative term of the same scaling:

- (a) $\text{Re}_\infty = M_\infty^2$ and $\text{Pé}_\infty = 1$
- (b) $\text{Re}_\infty = 1$ and $\text{Pé}_\infty = M_\infty^2$
- (c) $\text{Re}_\infty = \text{Pé}_\infty = M_\infty^2$

→ each of the above options will affect the other equations (mass and energy equations).

For a non-isentropic flow: mass equation

$$\partial_t \rho + \vec{\nabla} \cdot (\rho \vec{u}) = \frac{1}{\text{Pé}_\infty} \vec{\nabla} \cdot (\kappa \vec{\nabla} \rho)$$

choice (a) $\text{Pé}_\infty = 1$

$$\partial_t \rho + \vec{\nabla} \cdot (\rho \vec{u}) = \vec{\nabla} \cdot (\kappa \vec{\nabla} \rho)$$

→ the dissipative term is *well-scaled*

choice (b) and (c) $\text{Pé}_\infty = M_\infty^2$

$$\partial_t \rho + \vec{\nabla} \cdot (\rho \vec{u}) = \frac{1}{M_\infty^2} \vec{\nabla} \cdot (\kappa \vec{\nabla} \rho)$$

→ over-dissipation in the contact wave

Options (b) and (c) are not inappropriate. Thus, we are left with option (a): $\text{Re}_\infty = M_\infty^2$ and $\text{Pé}_\infty = 1$

For a non-isentropic flow: energy equation

$$\begin{aligned}\partial_{t^*} (\rho^* E^*) + \vec{\nabla}^* \cdot [\vec{u}^* (\rho^* E^* + P^*)] &= \frac{1}{\text{Pé}_\infty} \vec{\nabla}^* \cdot \left(\kappa^* \vec{\nabla}^* (\rho^* e^*) \right) \\ &+ \frac{M_\infty^2}{\text{Re}_\infty} \vec{\nabla}^* \cdot \left(\vec{u}^* \rho^* \mu^* \vec{\nabla}^{s,*} \vec{u}^* \right) + \frac{M_\infty^2}{2 \text{Pé}_\infty} \vec{\nabla}^* \cdot \left(\kappa^* (u^*)^2 \vec{\nabla}^* \rho^* \right)\end{aligned}$$

With option (a) it yields:

$$\begin{aligned}\partial_{t^*} (\rho^* E^*) + \vec{\nabla}^* \cdot [\vec{u}^* (\rho^* E^* + P^*)] &= \vec{\nabla}^* \cdot \left(\kappa^* \vec{\nabla}^* (\rho^* e^*) \right) \\ &+ \vec{\nabla}^* \cdot \left(\vec{u}^* \rho^* \mu^* \vec{\nabla}^{s,*} \vec{u}^* \right) + \frac{M_\infty^2}{2} \vec{\nabla}^* \cdot \left(\kappa^* (u^*)^2 \vec{\nabla}^* \rho^* \right)\end{aligned}$$

→ all dissipative terms are *well-scaled*.

For a non-isentropic flow: derivation of norm $_{P}^{\mu,\kappa}$

We derive the scaling of norm $_{P}^{\mu}$ and norm $_{P}^{\kappa}$ when $\text{Re}_{\infty} = M_{\infty}^2$ and $\text{Pé}_{\infty} = 1$:

Derive an expression for κ_{∞} :

$$\kappa_e(\vec{r}, t) = h^2 \frac{\max(\tilde{D}_e(\vec{r}, t), J)}{\text{norm}_{P}^{\kappa}} \rightarrow \kappa_{\infty} = \frac{\rho_{\infty} c_{\infty}^2 u_{\infty} L}{\text{norm}_{P,\infty}^{\kappa}}$$

Then, use the substitute the above expression for norm $_{P}^{\kappa}$ into Pé_{∞} to obtain:

$$\text{norm}_{P,\infty}^{\kappa} = \text{Pé}_{\infty} \rho_{\infty} c_{\infty}^2 = \rho_{\infty} c_{\infty}^2 \rightarrow \text{same as for low-Mach flows}$$

Same derivation using μ_e and Re_{∞} leads to:

$$\text{norm}_{P,\infty}^{\mu} = \text{Re}_{\infty} \rho_{\infty} c_{\infty}^2 = \rho_{\infty} u_{\infty}^2 \rightarrow \text{different from low-Mach flows}$$

How to merge the two cases?

$$\mu(\vec{r}, t) = \min \left(\mu_{\max}(\vec{r}, t), \mu_e(\vec{r}, t) \right) \text{ and } \kappa(\vec{r}, t) = \min \left(\mu_{\max}(\vec{r}, t), \kappa_e(\vec{r}, t) \right)$$

where $\kappa_{\max}(\vec{r}, t) = \mu_{\max}(\vec{r}, t) = \frac{h}{2} \left(\|\vec{u}\| + c \right)$.

$$\kappa_e(\vec{r}, t) = \frac{h^2 \max(\tilde{R}, J)}{\rho c^2} \text{ and } \mu_e(\vec{r}, t) = \frac{h^2 \max(\tilde{R}, J)}{\text{norm}_P^\mu}$$

where

$$\text{norm}_P^\mu = \mathbb{G}(M) \rho \|\vec{u}\|^2 + (1 - \mathbb{G}(M)) \rho c^2 \text{ and } \mathbb{G}(M) \lim_{M \rightarrow 0} 0$$

An example:

$$\mathbb{G}(M) = \frac{\tanh(a(M - M_\infty)) + |\tanh(a(M - M_\infty))|}{2}$$

$$J = \|\vec{u}\| \max \left([[\vec{\nabla} P \cdot \vec{n}]], c^2 [[\vec{\nabla} \rho \cdot \vec{n}]] \right)$$

Numerical results:

1-D converging-diverging nozzle

- steady-state solution and exact solution
- subsonic (liquid water) and supersonic (vapor) flows
- convergence study

2-D subsonic and transonic flows

- low-Mach flow over a cylinder: $M_{inlet} = 10^{-3}, 10^{-4}, 10^{-6}$ and 10^{-7}
- flow over a bump: $M_{inlet} = 0.7, 10^{-2}, 10^{-4}$ and 10^{-7}

2-D supersonic flow

Mach 2.5 flow over a forward facing step

1-D converging-diverging nozzle

Stiffened gas equation of state

$$P = (\gamma - 1)\rho(e - q) - \gamma P_\infty$$

Equation of state parameters

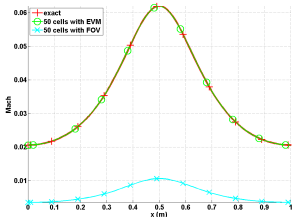
fluid	γ	$C_v \text{ (J.kg}^{-1}.\text{K}^{-1}\text{)}$	$P_\infty \text{ (Pa)}$	$q \text{ (J.kg}^{-1}\text{)}$
liquid water	2.35	1816	10^9	$-1167 \text{ } 10^3$
steam	1.43	1040	0	$2030 \text{ } 10^3$

Cross-section A

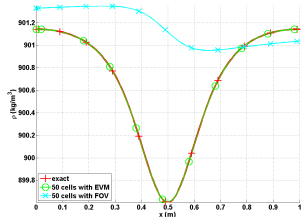
$$A(x) = 1 + 0.5 \cos(2\pi x)$$

- a steady state is reached
- low-Mach flow for liquid water
- supersonic flow for steam

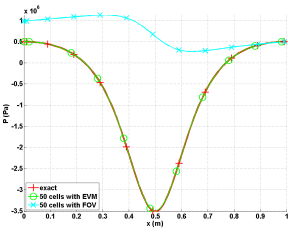
1-D converging-diverging nozzle: liquid water



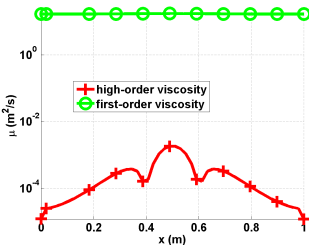
(e) Mach number



(f) Density



(g) Pressure



(h) Viscosity coefficients

1-D converging-diverging nozzle: liquid water

Convergence rates for the L_1 norm of the error:

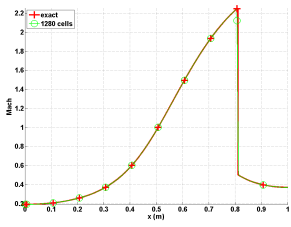
cells	density	rate	pressure	rate	velocity	rate
4	$2.8037 \cdot 10^{-1}$	—	$8.4705 \cdot 10^5$	—	7.2737	—
8	$1.3343 \cdot 10^{-1}$	0.495	$4.7893 \cdot 10^5$	0.24	6.1493	0.0747
16	$2.9373 \cdot 10^{-2}$	2.10	$1.0613 \cdot 10^5$	2.09	1.2275	2.25
32	$5.1120 \cdot 10^{-3}$	2.58	$1.8446 \cdot 10^4$	2.58	$1.8943 \cdot 10^{-1}$	2.78
64	$1.0558 \cdot 10^{-3}$	2.31	$3.7938 \cdot 10^3$	2.31	$3.7919 \cdot 10^{-2}$	2.37
128	$2.3712 \cdot 10^{-4}$	2.18	$8.4471 \cdot 10^2$	2.19	$8.5517 \cdot 10^{-3}$	2.17
256	$5.6058 \cdot 10^{-5}$	2.08	$1.9839 \cdot 10^2$	2.09	$2.0475 \cdot 10^{-3}$	2.07
512	$1.3278 \cdot 10^{-5}$	2.07	$4.6622 \cdot 10^1$	2.08	$4.9516 \cdot 10^{-4}$	2.06
1024	$3.1193 \cdot 10^{-6}$	—	$1.1755 \cdot 10^1$	—	$1.2379 \cdot 10^{-4}$	—

1-D converging-diverging nozzle: liquid water

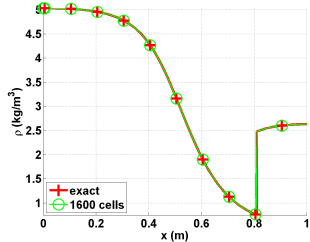
Convergence rates for the L_2 norm of the error:

cells	density	rate	pressure	rate	velocity	rate
4	$3.106397 \cdot 10^{-1}$	—	$5.254445 \cdot 10^5$	—	3.288543	—
8	$7.491623 \cdot 10^{-2}$	2.06	$1.636966 \cdot 10^5$	1.62	1.823880	0.14
16	$2.079858 \cdot 10^{-2}$	1.81	$4.627338 \cdot 10^4$	1.77	$4.990605 \cdot 10^{-1}$	1.83
32	$5.329627 \cdot 10^{-3}$	1.96	$1.180287 \cdot 10^4$	1.96	$1.261018 \cdot 10^{-1}$	1.98
64	$1.341583 \cdot 10^{-3}$	1.99	$2.967104 \cdot 10^3$	1.99	$3.160914 \cdot 10^{-2}$	1.99
128	$3.359766 \cdot 10^{-4}$	1.99	$7.428087 \cdot 10^2$	1.99	$7.907499 \cdot 10^{-3}$	1.99
256	$8.403859 \cdot 10^{-5}$	1.99	$1.857861 \cdot 10^2$	2.01	$1.977292 \cdot 10^{-3}$	2.00
512	$2.10075 \cdot 10^{-5}$	—	$4.7024 \cdot 10^1$	—	$4.9516 \cdot 10^{-4}$	—

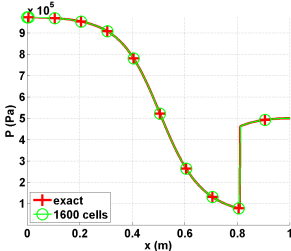
1-D converging-diverging nozzle: vapor



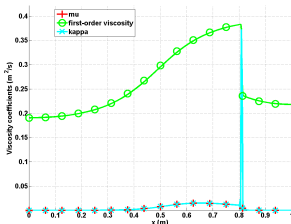
(i) Mach number



(j) Density



(k) Pressure



(l) Viscosity coefficients

1-D converging-diverging nozzle: vapor

Convergence rates for the L_1 norm of the error:

cells	density	rate	pressure	rate	velocity	rate
5	$0.72562 \cdot 10^{-1}$	—	$1.5657 \cdot 10^5$	—	173.69	—
10	$0.4165 \cdot 10^{-1}$	0.80088	$9.6741 \cdot 10^4$	0.63425	120.69	0.52519
20	$0.20675 \cdot 10^{-1}$	1.0104	$4.9193 \cdot 10^4$	0.96971	72.149	0.74228
40	$0.093703 \cdot 10^{-1}$	1.1417	$2.0103 \cdot 10^4$	0.72728	34.716	1.0554
80	$0.047328 \cdot 10^{-1}$	0.9854	$1.0208 \cdot 10^4$	0.9777	16.082	1.1101
160	$0.023965 \cdot 10^{-2}$	0.9817	$5.1969 \cdot 10^3$	0.9739	7.9573	1.0150
320	$0.020768 \cdot 10^{-2}$	0.9886	$2.5116 \cdot 10^3$	1.0490	3.7812	1.0734
640	$0.0059715 \cdot 10^{-2}$	1.0160	$1.2754 \cdot 10^3$	0.9776	1.8353	1.0428

1-D converging-diverging nozzle: vapor

Convergence rates for the L_2 norm of the error:

cells	density	rate	pressure	rate	velocity	rate
5	$9.7144 \cdot 10^{-1}$	—	$2.0215 \cdot 10^5$	—	236.94	—
10	$5.9718 \cdot 10^{-1}$	0.70195	$1.3024 \cdot 10^5$	0.63425	166.56	0.50854
20	$2.9503 \cdot 10^{-1}$	1.0173	$6.6503 \cdot 10^4$	0.96971	103.36	0.68831
40	$1.8193 \cdot 10^{-1}$	0.69747	$4.0171 \cdot 10^4$	0.72728	66.374	0.6390
80	$1.3366 \cdot 10^{-1}$	0.44485	$2.3163 \cdot 10^4$	0.43576	42.981	0.62692
160	$9.6638 \cdot 10^{-2}$	0.46790	$1.7263 \cdot 10^4$	0.42413	31.717	0.43844
320	$7.0896 \cdot 10^{-2}$	0.44688	$1.2763 \cdot 10^4$	0.43571	23.138	0.45499
640	$5.2191 \cdot 10^{-2}$	0.44190	$9.4217 \cdot 10^3$	0.43790	16.910	0.45238

2-D low-Mach flow over a cylinder

Typical benchmark problem for low-Mach flow:

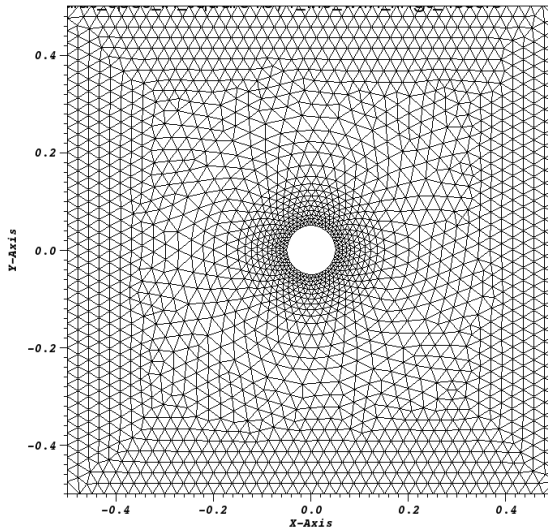
- The steady-state solution is symmetric: the iso-Mach contour lines are used to assess the symmetry of the numerical solution
- The velocity at the top of the cylinder is twice the incoming velocity set at the inlet
- The pressure fluctuations are proportional to the square of inlet Mach number, i.e.,

$$\delta P = \frac{\max(P(\vec{r})) - \min(P(\vec{r}))}{\max(P(\vec{r}))} \propto M_\infty^2$$

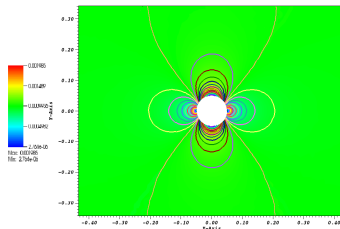
where δP and M_∞ denote the pressure fluctuations and the inlet Mach number, respectively.

- triangular mesh with 4008 triangular elements
- Ideal Gas equation of state with $\gamma = 1.4$
- CFL = 20

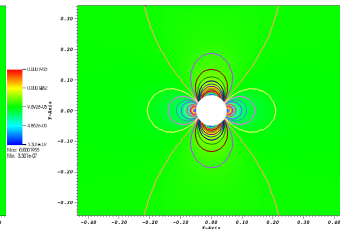
2-D low-Mach flow over a cylinder



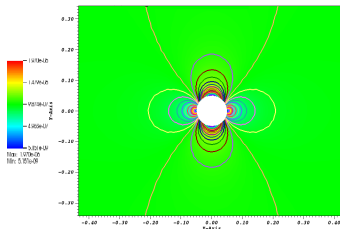
2-D low-Mach flow over a cylinder



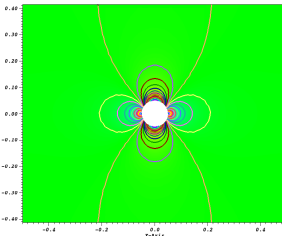
(m) $M_{\text{inlet}} = 10^{-3}$



(n) $M_{\text{inlet}} = 10^{-4}$

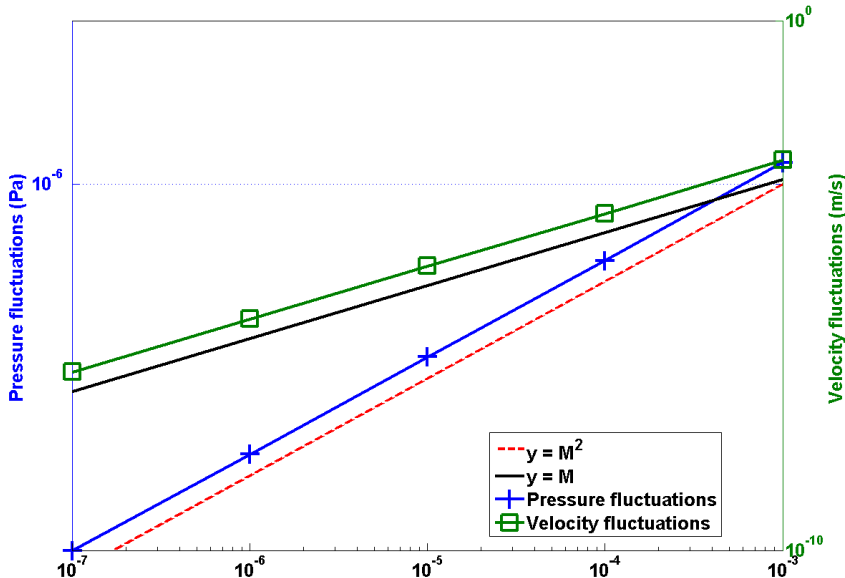


(o) $M_{\text{inlet}} = 10^{-6}$



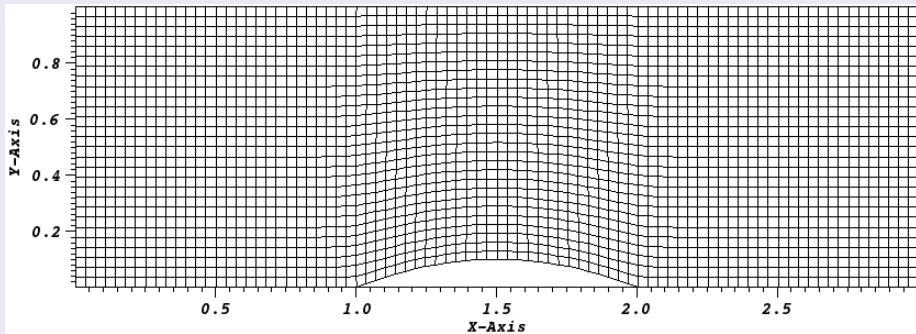
(p) $M_{\text{inlet}} = 10^{-7}$

2-D low-Mach flow over a cylinder



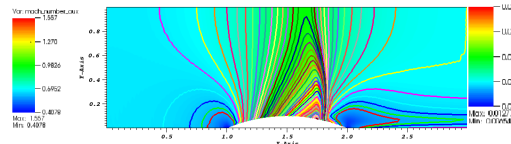
2-D low-Mach flow over a bump

Geometry: an uniform grid of 3352 Q_1 elements

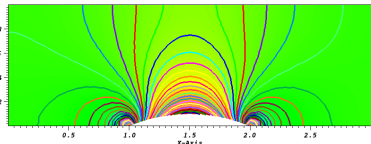


- Ideal Gas equation of state with $\gamma = 1.4$
- CFL = 20
- Inlet flow for different Mach numbers, static pressure and wall-boundary conditions.

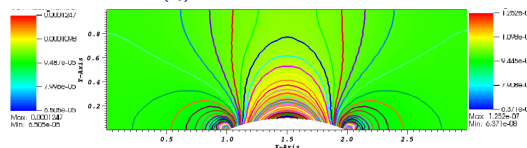
2-D low-Mach flow over a bump



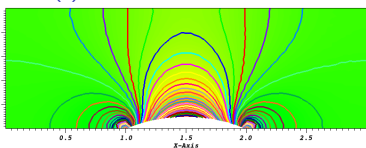
(q) $M_{\text{inlet}} = 0.7$



(r) $M_{\text{inlet}} = 10^{-2}$



$$(s) \quad M_{\text{inlet}} = 10^{-4}$$



$$(t) M_{\text{inlet}} = 10^{-7}$$

2-D Mach 2.5 flow over a forward facing step

The SEVEN-EquAtion Model with variable area (SEVEN-bandEd ArMadillo)



The seven-equation model (SEM)

The model

- Each phase obeys the single-phase Euler equations: two continuity equations, two momentum equations and two energy equations
- Seventh equation: void fraction equation → an internal boundary condition between the two phases at the interface
- Exchange terms between phases: relaxation terms. These terms were derived using *rational thermodynamic* → consistent with the entropy minimum principle
- **The system of equations is well-posed and has seven waves**
- The SEM degenerates to single-phase Euler equations when one phase disappears
- The SEM degenerates into a 5-equation model when using infinite relaxation coefficients

The seven-equation model (SEM)

Numerical stabilization methods

- discontinuous schemes (finite volume, DG)
- approximate Riemann solvers: HLL, HLLC with low-Mach fix
- apply upwind-type scheme for non-conservative flux

Our approach

- continuous scheme
- artificial dissipative method → EVM

The seven-equation model (SEM)

We consider two phases j, k . Phase k obeys the following system of equations:

$$\partial_t (\alpha_k A) + \vec{u}_{int} A \vec{\nabla} \alpha_k = A \mu_P (P_k - P_j)$$

$$\partial_t (\alpha_k \rho_k A) + \vec{\nabla} \cdot (\alpha_k \rho_k \vec{u}_k A) = 0$$

$$\begin{aligned} \partial_t (\alpha_k \rho_k \vec{u}_k A) + \vec{\nabla} \cdot [\alpha_k A (\rho_k \vec{u}_k \otimes \vec{u}_k)] + \vec{\nabla} (\alpha_k A P_k) = \\ \alpha_k P_k \vec{\nabla} A + P_{int} A \vec{\nabla} \alpha_k + A \lambda_u (\vec{u}_j - \vec{u}_k) \end{aligned}$$

$$\begin{aligned} \partial_t (\alpha_k \rho_k E_k A) + \vec{\nabla} \cdot [\alpha_k A \vec{u}_j (\rho_k E_k + P_k)] = \\ P_{int} \vec{u}_{int} A \vec{\nabla} \alpha_k - \mu_P \bar{P}_{int} (P_k - P_j) + \bar{u}_{int} A \lambda_u (\vec{u}_j - \vec{u}_k) \end{aligned}$$

$$\left\{ \begin{array}{l} P_{int} = \bar{P}_{int} - \frac{\vec{\nabla} \alpha_k}{||\vec{\nabla} \alpha_k||} \frac{Z_k Z_j}{Z_k + Z_j} \cdot (\vec{u}_k - \vec{u}_j) \\ \bar{P}_{int} = \frac{Z_k P_j + Z_j P_k}{Z_k + Z_j} \\ \vec{u}_{int} = \bar{\vec{u}}_{int} - \frac{\vec{\nabla} \alpha_k}{||\vec{\nabla} \alpha_k||} \frac{P_k - P_j}{Z_k + Z_j} \\ \bar{\vec{u}}_{int} = \frac{Z_k \vec{u}_k + Z_j \vec{u}_j}{Z_k + Z_j} \end{array} \right.$$

and $\left\{ \begin{array}{l} Z_k = \rho_k c_k \\ \mu_P = \frac{A_{int}}{Z_k + Z_j} \\ \lambda_u = \frac{\mu_P}{2} Z_k Z_j \\ A_{int} = 6.25 \cdot A_{int, max} \alpha_k (1 - \alpha_k)^2 \end{array} \right.$

The seven-equation model (SEM)

Methodology

- 1 derive the entropy equation WITHOUT the dissipative terms

$$(s_e)_k^{-1} \alpha_k \rho_k A \frac{ds_k}{dt} = \mu_P \frac{Z_k}{Z_k + Z_j} (P_j - P_k)^2 + \lambda_u \frac{Z_j}{Z_k + Z_j} (u_j - u_k)^2 \\ + \|\vec{\nabla} \alpha_k\| \frac{Z_k}{(Z_k + Z_j)^2} \left[Z_j (\vec{u}_j - \vec{u}_k) + \frac{\vec{\nabla} \alpha_k}{\|\vec{\nabla} \alpha_k\|} (P_k - P_j) \right]^2$$

- 2 same steps as for the multi-D Euler equations: recast the entropy residual, viscous regularization, non-dimensionalized equations, viscosity coefficients.

A particularity

Two phases \rightarrow two entropy residuals \rightarrow two options to derive the dissipative terms:

- (a) either we consider the total entropy residual by summing over the phases
- (b) or, we consider each phase independently of each other which will automatically ensure positivity of the total entropy

Viscous regularization for the multi-D SEM:

$$\partial_t (\alpha_k A) + \vec{u}_{int} A \vec{\nabla} \alpha_k = A \mu_P (P_k - P_j) + \vec{\nabla} \cdot \vec{l}_k$$

$$\partial_t (\alpha_k \rho_k A) + \vec{\nabla} \cdot (\alpha_k \rho_k \vec{u}_k A) = \vec{\nabla} \cdot \vec{f}_k$$

$$\begin{aligned} \partial_t (\alpha_k \rho_k \vec{u}_k A) + \vec{\nabla} \cdot [\alpha_k A (\rho_k \vec{u}_k \otimes \vec{u}_k + P_k \mathbb{I})] = \\ \alpha_k P_k \vec{\nabla} A + P_{int} A \vec{\nabla} \alpha_k + A \lambda_u (\vec{u}_j - \vec{u}_k) + \vec{\nabla} \cdot \vec{g}_k \end{aligned}$$

$$\begin{aligned} \partial_t (\alpha_k \rho_k E_k A) + \vec{\nabla} \cdot [\alpha_k A \vec{u}_j (\rho_k E_k + P_k)] = \\ P_{int} \vec{u}_{int} A \vec{\nabla} \alpha_k - \mu_P \bar{P}_{int} (P_k - P_j) + \bar{\vec{u}}_{int} A \lambda_u (\vec{u}_j - \vec{u}_k) + \vec{\nabla} \cdot \vec{h}_k \end{aligned}$$

$$\left\{ \begin{array}{l} \vec{l}_k = ? \\ \vec{f}_k = \alpha_k A \kappa_k \vec{\nabla} \rho_k + \rho_k \vec{l}_k \\ \vec{g}_k = \alpha_k A \rho_k \mu_k \vec{\nabla}^s \vec{u}_k + \vec{u}_k \otimes \vec{f}_k \\ \vec{h}_k = \alpha_k A \kappa_k \vec{\nabla} (\rho_k e_k) - \frac{\|\vec{u}_k\|^2}{2} \vec{f}_k + \vec{u} \cdot \vec{g}_k + \rho_k e_k \vec{l}_k \end{array} \right.$$

How to derive the dissipative term \vec{I} ?

$$\partial_t (\alpha_k A) + A \vec{u}_{int} \cdot \vec{\nabla} \alpha_k = \vec{\nabla} \cdot \vec{I}_k$$

- scalar hyperbolic equation with eigenvalue \vec{u}_{int}
- by analogy to the Burger's equation $\rightarrow \vec{I}_k = A \beta_k \vec{\nabla} \alpha_k$
- this regularization ensures positivity of α_k
- β_k is a positive viscosity coefficient:

$$\beta_k = \min(\beta_{k,e}, \beta_{max}) \text{ where}$$

$$\beta_{max} = \frac{h}{2} \|\vec{u}_{int}\| \text{ and } \beta_{k,e} = h^2 \frac{\max(R_\alpha, J_\alpha)}{\|\eta - \bar{\eta}\|_\infty}$$

$$R_\alpha = \partial_t \eta + \vec{u}_{int} \cdot \vec{\nabla} \eta \text{ with } \eta = \frac{\alpha_k^2}{2}$$

→ when assuming $\mu_k = \kappa_k = \beta_k$, the parabolic regularization is retrieved

What about the viscosity coefficients μ_k and κ_k ?

Same as single-phase equations

1-D shock tube

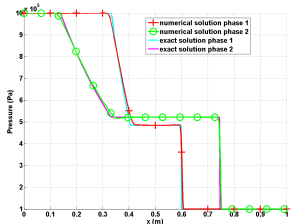
- two independent fluids
- two fluids with pressure and velocity relaxation terms

1-D shock tube with two independent fluids

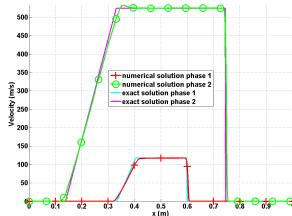
- two fluids (1 and 2) described with ideal gas equation of state: $P = (\gamma - 1)\rho e$
- heavy fluid with $\gamma_1 = 3$ and light fluid with $\gamma_2 = 1.4$
- no interaction between the two fluids ($\mu_P = \lambda_u = 0$) \rightarrow same as running a single-phase flow code twice
- exact solution is available and obtained from a Riemann solver
- 500 cells, $CFL = 1$ and $t_{final} = 305\mu s$
- initial step pressure: $P_{left} = 1\text{ MPa}$ and $P_{right} = 0.1\text{ MPa}$
- fluids are initially at rest and uniform volume fraction $\alpha_i = 0.5$
- uniform initial density $\rho_1 = 10\text{ kg} \cdot \text{m}^{-3}$ and $\rho_2 = 1\text{ kg} \cdot \text{m}^{-3}$

Objective: verify that the dissipative terms does not affect the volume fraction profile

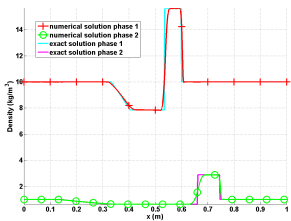
1-D shock tube with two independent fluids



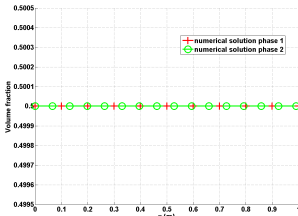
(u) Pressure at $t = 305 \mu s$



(v) Velocity at $t = 305 \mu s$

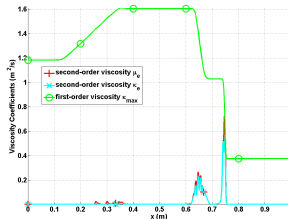


(w) Density at $t = 305 \mu s$



(x) Volume fraction at $t = 305 \mu s$

1-D shock tube with two independent fluids



(y) Viscosity coefficients phase 1 (z) Viscosity coefficients phase 2

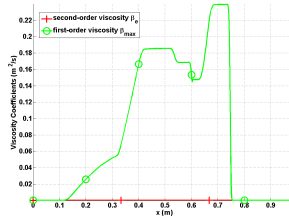
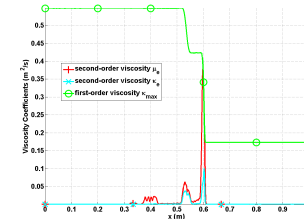


Figure: Viscosity coefficients volume fraction

1-D shock tube with infinite relaxation coefficients

- same fluids, same initial conditions and same equation of state
- relaxation parameters are turned on and computed with $A_{int,max} = 10^4 \text{ m}^{-1}$

$$\mu_p = \frac{A_{int}}{Z_1 + Z_2}$$

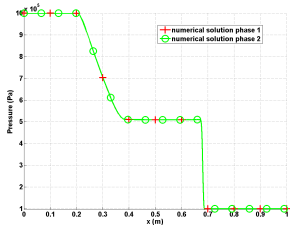
$$\lambda_u = \frac{\mu_p}{2} Z_1 Z_2$$

$$A_{int} = A_{int,max}$$

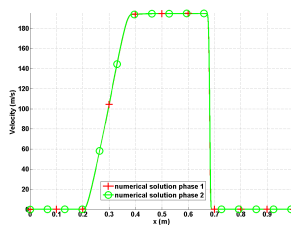
- volume fraction will vary because of the pressure relaxation term
- NO exact solution available

Objective: verify that the volume fraction is correctly stabilized by the EVM

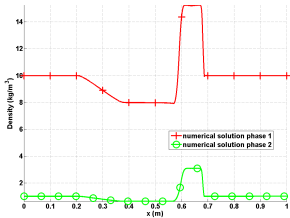
1-D shock tube with infinite relaxation coefficients



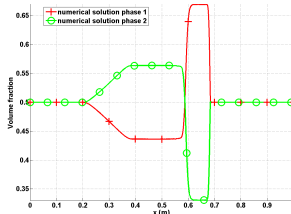
(a) Pressure at $t = 305 \mu s$



(b) Velocity at $t = 305 \mu s$



(c) Density at $t = 305 \mu s$



(d) Volume fraction at $t = 305 \mu s$

1-D shock tube with infinite relaxation coefficients

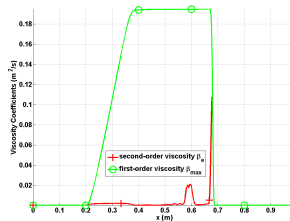
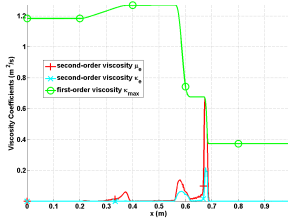
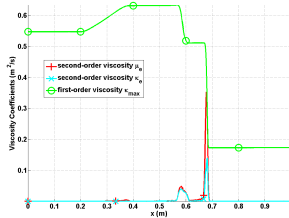


Figure: Viscosity coefficients volume fraction

Conclusions and future work

The multi-D Euler equations with variable area

- extended the viscous regularization to Euler equation with variable area
- extended the EVM to low-Mach flows by doing a low-Mach asymptotic limit
→ worked with non-dimensionalized equations
- validated our approach with 1 and 2-D simulations and convergence tests
- applied the EVM with the Stiffened Gas equation of state

The seven equation model (SEM)

- derived a viscous regularization for the SEM
- defined the viscosity coefficients using the same methodology as for single-phase flow equation
- our approach was validated by 1-D results

Future work

Use the viscous regularization for the SEM to run 2-D simulations → require a preconditioner

The 1-D Radiation-Hydrodynamic Equation (RHEA)



QUESTIONS/COMMENTS ?

1-D Euler equations numerical results

An other normalization function for μ_e

$$\mu_e = h^2 \frac{\max(|\tilde{R}|, J_P)}{\text{norm}_P^\mu}$$

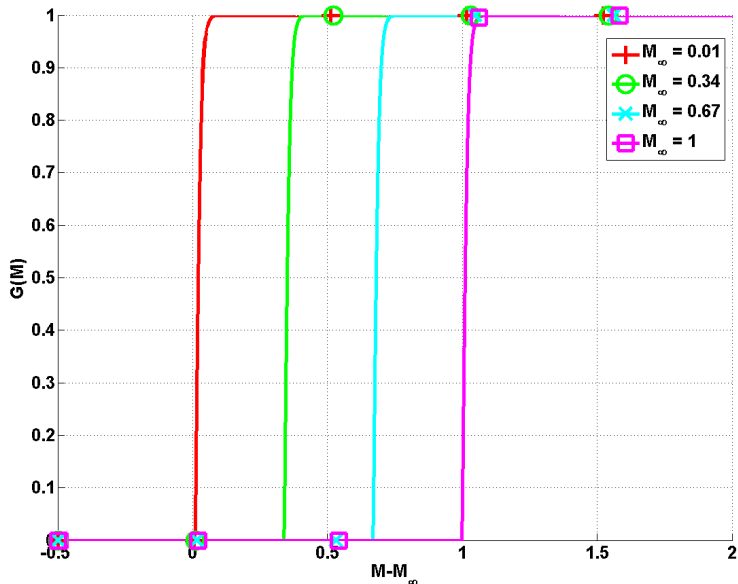
$$\text{norm}_P^\mu = (1 - \mathbb{G}(M))\rho c^2 + \mathbb{G}(M)\rho ||\vec{u}||^2 \text{ where } \lim_{M \rightarrow 0} \mathbb{G} = 0$$

Example

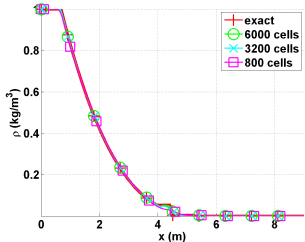
$$\mathbb{G}(M) = \frac{\tanh(a(M - M_\infty)) + |\tanh(a(M - M_\infty))|}{2}$$

a and M_∞ are two constants to set

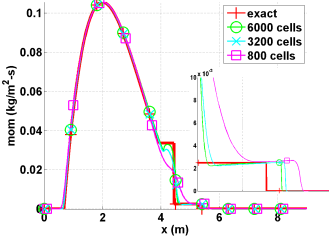
$$a = 10$$



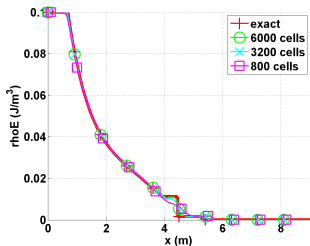
Leblanc shock tube



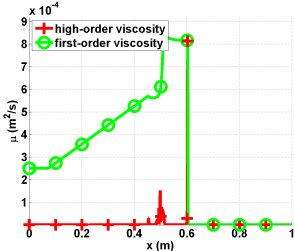
(a) Density



(b) Momentum

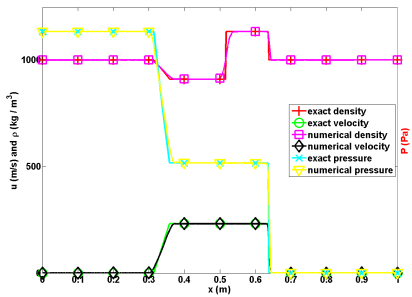


(c) Total energy

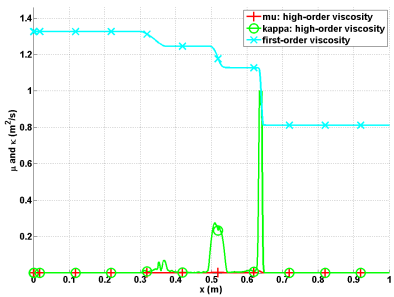


(d) Viscosity coefficients

Shock tube for liquid phase

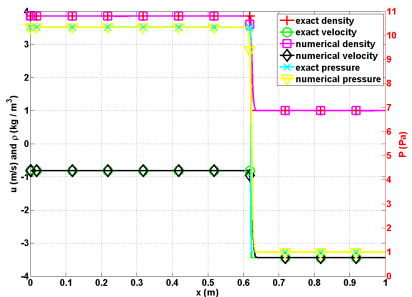


(e) Density, velocity and pressure profiles.

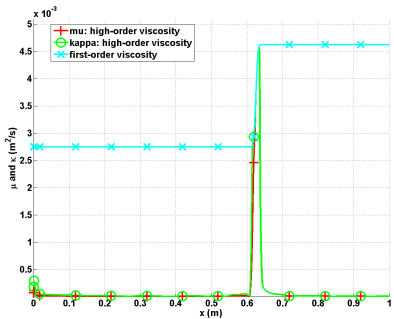


(f) Viscosity coefficients profile.

Slow moving shock

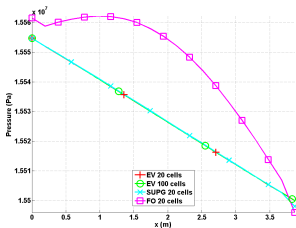


(g) Velocity, density and pressure

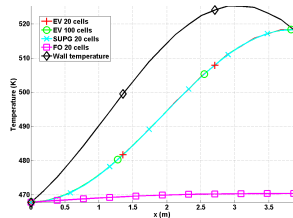


(h) Viscosity coefficients

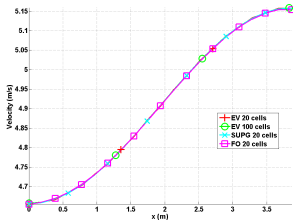
PWR



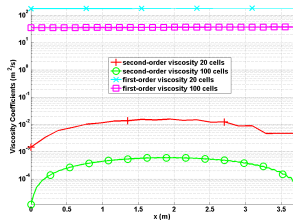
(i) Axial pressure profile



(j) Axial temperature profile



(k) Axial velocity profile



(I) Axial viscosity profile

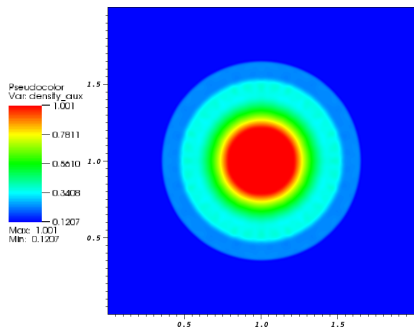
2-D Euler equations numerical results

2-D low-Mach flow over a cylinder

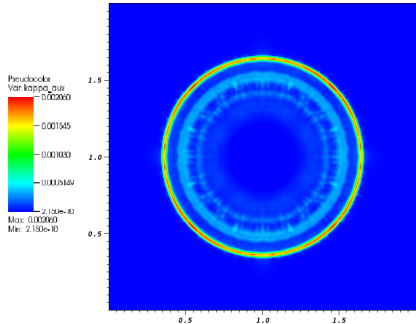
Velocity ratio for different Mach numbers

Mach number	inlet velocity	velocity at the top of the cylinder	ratio
10^{-3}	$2.348 \cdot 10^{-3}$	$1.176 \cdot 10^{-3}$	1.99
10^{-4}	$2.285 \cdot 10^{-4}$	$1.145 \cdot 10^{-4}$	1.99
10^{-5}	$2.283 \cdot 10^{-5}$	$1.144 \cdot 10^{-5}$	1.99
10^{-6}	$2.283 \cdot 10^{-6}$	$1.144 \cdot 10^{-6}$	1.99
10^{-7}	$2.283 \cdot 10^{-7}$	$1.144 \cdot 10^{-7}$	1.99

2-D explosion: solution at $t = 0.2$ s



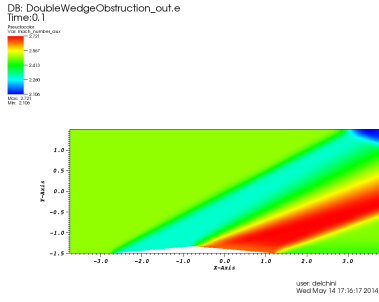
(m) Density



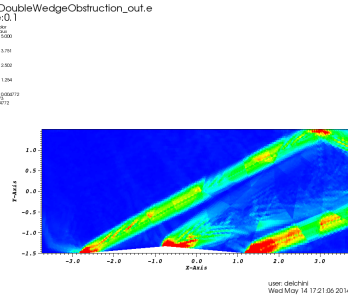
(n) Viscosity coefficient

2-D compression corner

Supersonic flow over a 5° double-wedge obstruction



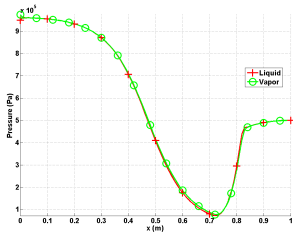
(o) Pressure



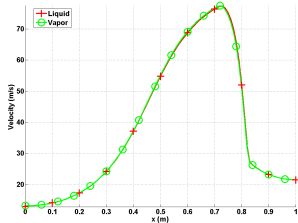
(p) Viscosity coefficient

Seven equation model

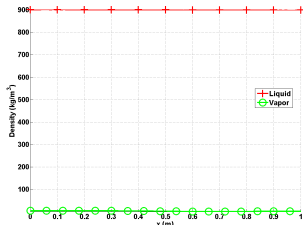
1-D converging-diverging nozzle with relaxation terms



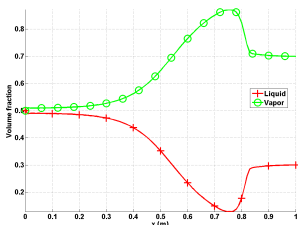
(q) Pressure



(r) Velocity

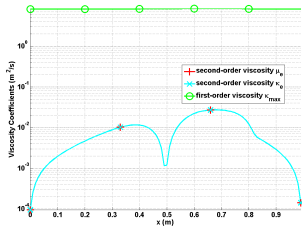


(s) Density

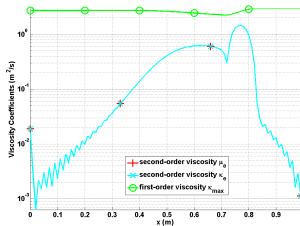


(t) Volume fraction

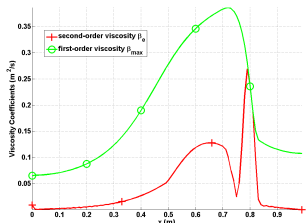
1-D converging-diverging nozzle with relaxation terms



(u) Liquid water

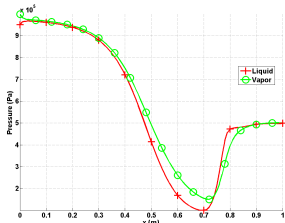


(v) Vapor

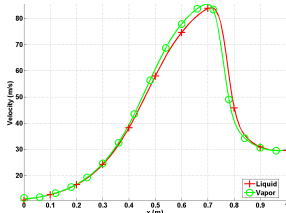


(w) β

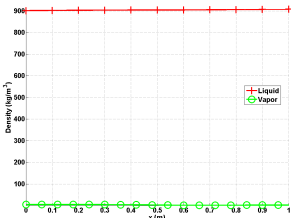
1-D converging-diverging nozzle with all source terms



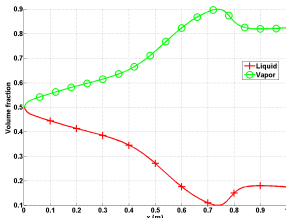
(x) Pressure



(y) Velocity

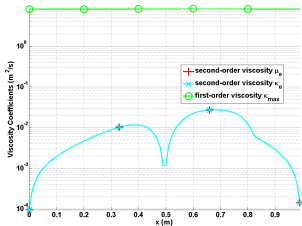


(z) Density

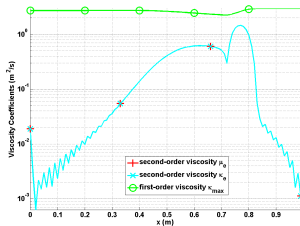


() Volume fraction

1-D converging-diverging nozzle with all source terms



(a) Liquid water



(b) Vapor

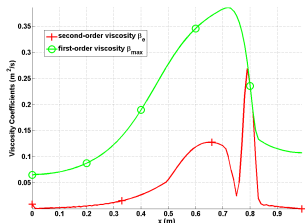


Figure: β

1-D Grey Radiation-Hydrodynamic equations

Equations

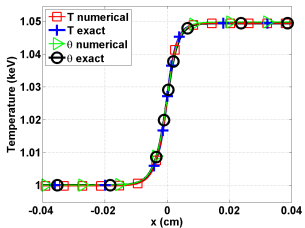
$$\partial_t(\rho) + \partial_x(\rho u) = \partial_x(\kappa \partial_x \rho)$$

$$\partial_t(\rho u) + \partial_x \left(\rho u^2 + P + \frac{\epsilon}{3} \right) = \partial_x(\kappa \partial_x \rho u)$$

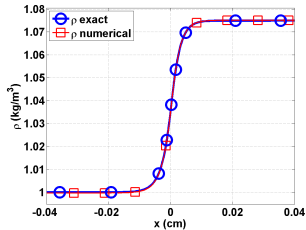
$$\partial_t(\rho E) + \partial_x [u(\rho E + P)] + \frac{u}{3} \partial_x \epsilon = \partial_x(\kappa \partial_x(\rho E))$$

$$\partial_t \epsilon + \frac{4}{3} \partial_x(u \epsilon) - \frac{u}{3} \partial_x \epsilon = \partial_x(\kappa \partial_x \epsilon)$$

Steady-state solution for Mach 1.05



(a) Temperatures.



(b) Material density.

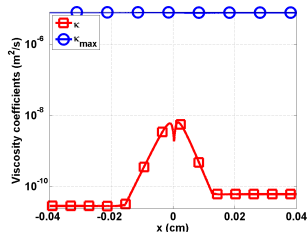
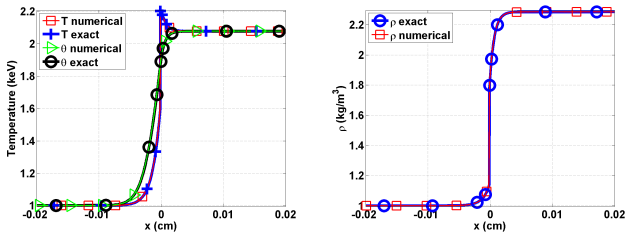


Figure: Viscosity coefficients

Steady-state solution for Mach 2



(a) Temperatures.

(b) Material density.

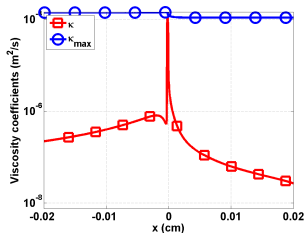
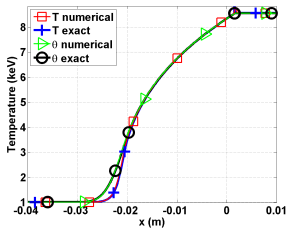
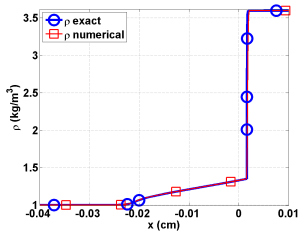


Figure: Viscosity coefficients

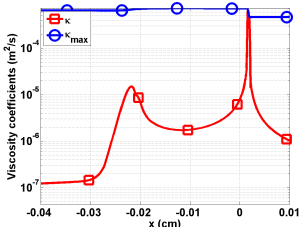
Steady-state solution for Mach 5



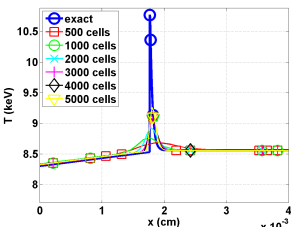
(a) Temperatures.



(b) Material density.

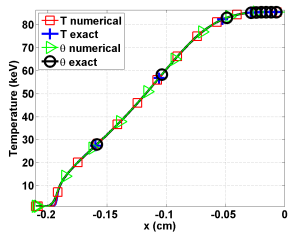


(c) Viscosity coefficients.

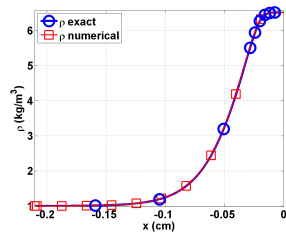


(d) Location of the peak.

Steady-state solution for Mach 50



(e) Temperatures.



(f) Material density.

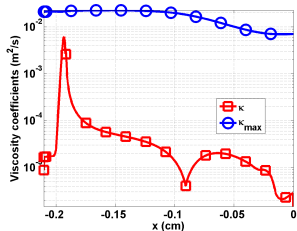


Figure: Viscosity coefficients